Granick, S., & Mauzerall, D. (1958) *J. Biol. Chem. 232*, 1119-1140.
Jaffe, E. K., & Hanes, D. (1986) *J. Biol. Chem. 261*, 9348-9353.
Jaffe, E. K., & Markham, G. D. (1987) *Biochemistry 26*, 4258-4264.
Jaffe, E. K., & Rajagopalan, J. S. (1990) *Bioorg. Chem. 18*, 381-394.
Jaffe, E. K., Salowe, S. P., Chen, N. T., & Dehaven, P. (1984) *J. Biol. Chem. 259*, 5032-5036.
Jaffe, E. K., Markham, G. D., & Rajagopalan, J. S. (1990) *Biochemistry 29*, 8345-8350.
Jordan, P. M., & Seehra, J. S. (1980) *J. Chem. Soc., Chem. Commun.*, 240-242.
Li, J. M., Russell, C. S., & Cosloy, S. D. (1989) *Gene 75* (1), 177-184.
Means, G. E., & Feeney, R. E. (1990) *Bioconjugate Chem. 1*, 2-12.
Myers, A. M., Crivellone, M. D., Koerner, T. J., & Tzagoloff, A. (1987) *J. Biol. Chem. 262*, 16822-16829.
Nandi, D. L., & Shemin, D. (1968) *J. Biol. Chem. 243*, 1236-1242.
Pappin, D. J. C., Coull, J. M., & Koester, H. (1990) in *Current Research in Protein Chemistry: Techniques, Structure & Function, New Approaches to Covalent Sequence Analysis* (Villafranca, J. J., Ed.) pp 191-202, Academic Press, New York.
Penning, T. M., Abrams, W. R., & Paulowski, J. E. (1991) *J. Biol. Chem.* (in press).
Seehra, J. S., & Jordan, P. M. (1981) *Eur. J. Biochem. 113*, 435-446.
Schoellmann, G., & Shaw, E. (1963) *Biochemistry 2*, 252-255.
Shemin, D., & Russell, C. S. (1953) *J. Am. Chem. Soc. 75*, 4873.
Smith, D. J., Maggio, E. T., & Kenyon, G. L. (1975) *Biochemistry 14*, 766-771.
Vallee, B. L., & Auld, D. S. (1990) *Biochemistry 29*, 5647-5659.
Wetmer, J. G., Bishop, D. F., Cantelmo, C., & Desnick, R. J. (1987) *Proc. Natl. Acad. Sci. U.S.A. 83*, 7703-7707.

Kinetic Method for Differentiating Mechanisms for Ligand Exchange Reactions: Application To Test for Substrate Channeling in Glycolysis

Xiaomao Wu,[‡] H. Gutfreund,[§] and P. B. Chock*[,‡]

Laboratory of Biochemistry, National Heart, Lung and Blood Institute, National Institutes of Health, Bethesda, Maryland 20892, and Department of Biochemistry, University of Bristol, Bristol, U.K.

Received July 22, 1991; Revised Manuscript Received October 21, 1991

ABSTRACT: We have derived analytical expressions for the kinetics of the two mechanisms involved in ligand substitution reactions. These mechanisms are (i) a dissociative mechanism in which the leaving ligand is first dissociated prior to the binding of the incoming ligand and (ii) an associative mechanism where a ternary complex is formed between the incoming ligand and the complex containing the leaving ligand. The equations obtained provide the theoretical basis for differentiating these two mechanisms on the basis of their kinetic patterns of the displacement reactions. Analysis of these equations shows that an associative mechanism can only generate an increasing kinetic pattern for the observed pseudo-first-ordered rate constants as a function of increasing concentration of the incoming ligand and plateaus, in most cases, at a value higher than the off-rate constant of the leaving ligand. However, a dissociative mechanism can generate either an increasing or a decreasing (k_{app} decreases with increasing concentrations of the incoming ligand) kinetic pattern, depending on the magnitudes of the individual rate constants involved, and, in either case, it will plateau at k_{app} equal to the k_{off} of the leaving ligand. Therefore, the decreasing kinetic pattern is a hallmark for a dissociative mechanism. This general method was used to settle the dispute of whether NADH is transferred directly via the enzyme–enzyme complex between glycerol-3-phosphate dehydrogenase (GPDH; EC 1.1.1.8) and L-lactate dehydrogenase (LDH; EC 1.1.1.27). Evidence for direct transfer of this metabolite between these two enzymes has been claimed and used to support substrate channeling in glycolysis [Srivastava, D. K., & Bernhard, S. A. (1987) *Biochemistry 26*, 1240-1246; Srivastava, D. K., Smolen, P., Betts, G. F., Fukushima, T., Spivey, H. O., & Bernhard, S. A. (1989) *Proc. Natl. Acad. Sci. U.S.A. 86*, 6464-6468]. Reexamination of this evidence reveals that the conclusion is based on misinterpretation of the kinetics of ligand exchange [Chock, P. B., & Gutfreund, H. (1988) *Proc. Natl. Acad. Sci. U.S.A. 85*, 8870-8874]. Application of this method to analyze the displacement data from our laboratory and those reported by Srivastava et al. (1989) confirms that NADH transfer between its complex with GPDH and with LDH proceeds via a dissociative mechanism. This is consistent with the transient kinetic and sedimentation equilibrium data reported by Wu et al. [Wu, X., Gutfreund, H., Lokatos, S., & Chock, P. B. (1991) *Proc. Natl. Acad. Sci. U.S.A. 88*, 497-501].

Substrate channeling, where the product of the reaction catalyzed by one enzyme is directly transferred via a multienzyme complex to a second enzyme to be used as its substrate, has been proposed for the glycolytic pathway (Srivastava & Bernhard, 1986a,b). Among the supporting evidence claimed is the kinetic data showing that NADH is transferred directly between its complexes with glycerol-3-phosphate dehydrogenase (GPDH, EC 1.1.1.8) and with lactate de-

* To whom correspondence should be addressed.
[‡] NHLBI, NIH.
[§] University of Bristol.

This article not subject to U.S. Copyright. Published 1992 by the American Chemical Society

hydrogenase (LDH, EC 1.1.1.27) (Srivastava & Bernhard, 1986a, 1987). This nucleotide-transfer reaction can be easily monitored by the large change in fluorescence excitation and emission spectra. Chock and Gutfreund (1988) showed that Srivstava and Bernhard's interpretation of kinetic data was flawed. Srivastava et al. (1989) responded with a revision of their own and criticism of our data. To further clarify this problem, we reported (Wu et al., 1991) the results of detailed kinetic studies on NADH binding on GPDH and LDH, and on the displacement of the NADH-bound enzyme by LDH or GPDH. In addition, we (Wu et al., 1991) showed by sedimentation equilibrium and gel filtration experiments that LDH and GPDH do not form complexes in the presence of saturating NADH concentration. Together, our data demonstrate that GPDH and LDH do not form multienzyme complexes and the transfer of NADH between these enzymes proceeds via a dissociative mechanism.

We report here a clear-cut method to differentiate between a dissociative and an associative mechanism in ligand displacement reactions. The two mechanisms in question are (1) dissociative mechanism (free diffusion)

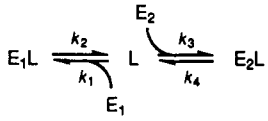

(1)

and (2) associative mechanism (direct transfer or substrate channeling)

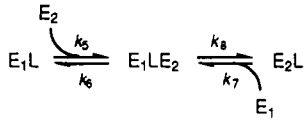

(2)

where E_1 and E_2 represent enzymes 1 and 2 or displaced and displacing reagents, respectively, and L denotes ligand or acceptor of the displacement reagents. In this report we will demonstrate, using analytical solutions, that the two mechanisms in question can be differentiated by their kinetic patterns.

Theoretical Treatment

The net reaction described in eqs 1 and 2 is

$$E_1L + E_2 \rightleftharpoons E_2L + E_1 \quad (3)$$

The rates of this displacement reaction can be monitored under pseudo-first-order conditions, i.e., $[E_1L]_o \ll [E_2]_o$.[1] The rate constants k_{app} so obtained can be plotted as a function of $[E_2]_o$. As described below, this kinetic pattern can be used to differentiate the two mechanisms described in eqs 1 and 2. Both numerical and analytical solutions are presented.

The numerical analysis is carried out by solving the differential equations describing the mechanism being considered using the integrator of the MLAB software package, which uses a combined Adams–Gear method (Knott, 1979) (Civilized Software, Inc., Bethesda, MD).

Dissociative Mechanism. When reaction 3 proceeds via a dissociative mechanism, and $[E_2]_o$ is much larger than $[E_1L]_o$, $[E_2]_o \simeq [E_2]$. It follows that

$$\frac{d[L]}{dt} = -(k_1[E_1]_o + k_3[E_2]_o + k_4)[L] + (k_2 - k_4)[E_1L] + k_1[L][E_1L] + k_4[L]_o \quad (4)$$

$$\frac{d[E_1L]}{dt} = k_1[E_1]_o[L] - k_2[E_1L] - k_1[L][E_1L] \quad (5)$$

[1] The symbols $[A]_o$, $[A]_e$, and $[A]$ represent the total, equilibrium, and free concentrations of A, respectively.

At equilibrium

$$K_1 = \frac{[L]_e[E_1]_e}{[E_1L]_e} = \frac{k_2}{k_1}$$

$$K_2 = \frac{[L]_e[E_2]_o}{[E_2L]_e} = \frac{k_4}{k_3}$$

Let us define the deviation from equilibrium as x and y for L and E_1L such that

$$x = [L]_e - [L]$$

$$y = [E_1L]_e - [E_1L]$$

From eqs 4 and 5, we obtain

$$\frac{dx}{dt} = -(k_1[E_1]_o + k_3[E_2]_o + k_4 - k_1[E_1L]_e)x + (k_2 - k_4 + k_1[L]_e)y + k_1xy \quad (6)$$

$$\frac{dy}{dt} = k_1([E_1]_o - [E_1L]_e)x - (k_2 + k_1[L]_e)y - k_1xy \quad (7)$$

When the deviation from equilibrium is small such that the nonlinear term, xy, is negligible, one can solve eqs 6 and 7 to yield a two-term exponential function as their solutions

$$F(t) + C_+e^{-k_+t} + C_-e^{-k_-t}$$

with C_+ and C_- as coefficients and the two rate constants given by

$$k_\pm = \frac{1}{2}[(\gamma_1 + \gamma_2 + \gamma_3) \pm \sqrt{(\gamma_1 + \gamma_2 + \gamma_3)^2 - 4(\gamma_1k_4 + \gamma_2\gamma_3)}] \quad (8)$$

where

$$\gamma_1 = k_1([E_1]_o - [E_1L]_e)$$

$$\gamma_2 = k_3[E_2]_o + k_4$$

$$\gamma_3 = k_2 + k_1[L]_e$$

The equilibrium concentrations of E_1L and L are given by

$$[E_1L]_e = \frac{1}{2}\left[[L]_o + [E_1]_o + K_1\left(1 + \frac{[E_2]_o}{K_2}\right) - \sqrt{\left[[L]_o + [E_1]_o + K_1\left(1 + \frac{[E_2]_o}{K_2}\right)\right]^2 - 4[L]_o[E_o]}\right] \quad (9)$$

$$[L]_e = ([L]_o - [E_1L]_e)/\left(1 + \frac{[E_2]_o}{K_2}\right) \quad (10)$$

Equations 9 and 10 show that when $[E_2]_o \rightarrow \infty$, $[E_1L]_e$ and $[L]_e$ approach zero or all of the L will be bound to E_2. Under these conditions, k_+ is approximately proportional to $[E_2]_o$ with a coefficient of k_3. In contrast, k_- has k_2 as its limiting value. On the basis of the time range of our kinetic measurement which monitored the substitution and not the fast initial ligand-binding step, k_{app} correspondings to k_-. By subtracting k_2 from each side of k_- expression in eq 8 one obtains a rearranged equation

$$k_- - k_2 = \frac{1}{2}[(\gamma_1 + \gamma_2 + \gamma_3 - 2k_2) - \sqrt{(\gamma_1 + \gamma_2 + \gamma_3 - 2k_2)^2 - 4k_1\delta}] \quad (11)$$

where

$$\delta = (k_4 - k_2)([E_1]_o + [L]_e - [E_1L]_e) + k_3[E_2]_o[L]_e \quad (12)$$

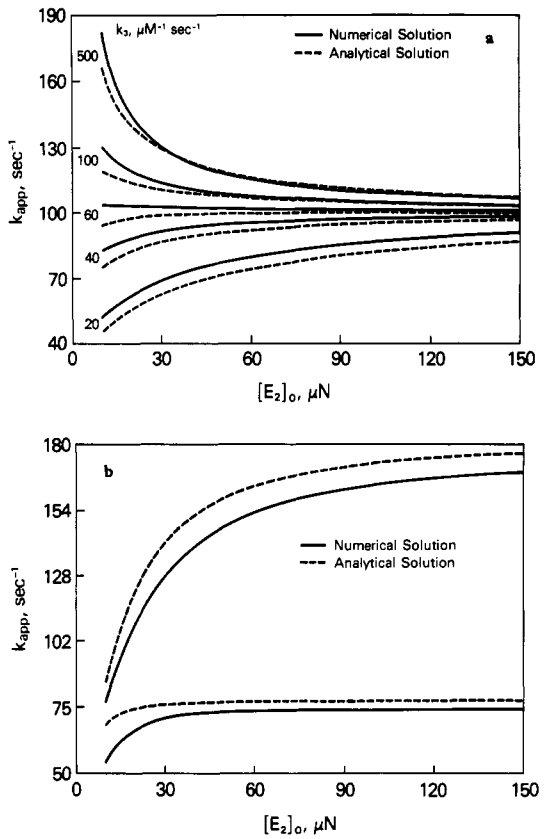

FIGURE 1: Comparison between numerical and analytical solutions. (a) Dissociative mechanism: $k_1 = 100\ \mu M^{-1}\ s^{-1}$, $k_2 = 100\ s^{-1}$, and $k_4/k_3 = 1\ \mu M$ with k_3 being varied from 20 (bottom) to 500 (top) $\mu M^{-1}\ s^{-1}$. Solid curves are from the numerical solution with $[E_1] = 3.589$, $[E_1L] = 3.911$, $[L] = 1.089$, and $[E_2L] = 0\ \mu M$ at $t = 0$. The dashed curves were for k_- calculated using eq 8 with $[E_1]_o = 7.5$ and $[L]_o = 5\ \mu M$. (b) Associative mechanism: $k_5 = k_7 = 10\ \mu M^{-1}\ s^{-1}$, $k_6 = k_8 = 20$ (lower curves) or $100\ s^{-1}$ (upper curves). Solid curves are from the numerical solution with $[E_1L] = 3.911$, $[E_1] = 3.589$, and $[E_1LE_2] = [E_2L] = 0\ \mu M$ at $t = 0$. The dashed curves were calculated using eq 18 with $[E_1]_o = 7.5$ and $[L]_o = 7.5\ \mu M$.

Equation 11 and δ have the same sign. When $k_4 \geq k_2$, then $\delta > 0$, or $k_- > k_2$. In other words, the values of k_{app} decreases and approaches k_2 as $[E_2]_o$ approaches ∞. When $k_4 < k_2$, δ can either be + or −, depending on the relative values between the first and second terms in eq 12. By setting $\delta = 0$ and $[E_2]_o \rightarrow \infty$, one obtains a critical boundary such that $k_4^c = k_2[E_1]_o/([E_1]_o + [L]_o)$. When $k_4 > k_4^c$, $\delta > 0$, then k_- decreases to k_2 as $[E_2]_o$ increases. However, if $k_4 < k_4^c$, $\delta < 0$ and k_- increases to k_2 as $[E_2]_o$ increases. This variation of kinetic patterns is illustrated in Figure 1a.

Associative Mechanism. When the reaction proceeded via an associative mechanism and $[E_2]_o \gg [E_1L]_o$, based on the reaction scheme shown in eq 2, we have

$$\frac{d[E_1L]}{dt} = -k_5[E_2]_o[E_1L] + k_6[E_1LE_2] \quad (13)$$

$$\frac{d[E_1LE_2]}{dt} = [k_5[E_2]_o - k_7([E_1]_o + [L]_o)][E_1L] - [k_6 + k_8 + k_7([E_1]_o + [L]_o)][E_1LE_2] + k_7([E_1L] + [E_1LE_2])^2 + k_7[E_1]_o[L]_o \quad (14)$$

Similar to the dissociative mechanism, one can define the dissociation constants K_3 and K_4 and the deviation from equilibrium as u and v for E_1L and E_1LE_2, respectively, such that

$$K_3 = \frac{[E_2]_o[E_1L]_e}{[E_1LE_2]_e} = \frac{k_6}{k_5}$$

$$K_4 = \frac{[E_1]_e[E_2L]_e}{[E_1LE_2]_e} = \frac{k_8}{k_7}$$

$$u = [E_1L]_e - [E_1L]$$

$$v = [E_1LE_2]_e - [E_1LE_2]$$

From eqs 13 and 14, one obtains

$$\frac{du}{dt} = -k_5[E_2]_o u + k_6 v \quad (15)$$

$$\frac{dv}{dt} = k_5[E_2]_o - k_7\epsilon u - (k_6 + k_8 + k_7\epsilon)v + k_7(u + v)^2 \quad (16)$$

where

$$\epsilon = [E_1]_o + [L]_o - 2([E_1L]_e + [E_1LE_2]_e) \quad (17)$$

When the deviation from the equilibrium state is sufficiently small, one can neglect the nonlinear term in eq 16. Under these conditions, with the same method described for the dissociative mechanism, one obtained

$$k_\pm = \frac{1}{2}[(k_5[E_2]_o + k_6 + k_8 + k_7\epsilon) \pm \sqrt{(k_5[E_2]_o + k_6 - k_8 - k_7\epsilon)^2 + 4k_6k_8}] \quad (18)$$

Equation 17 can be expressed in terms of $[E_1]_o$ and $[L]_o$, and for simplicity let

$$Q = \frac{K_4[E_2]_o}{K_3 + [E_2]_o}$$

then eq 17 becomes

$$\epsilon = \sqrt{([E_1]_o + [L]_o + Q)^2 - 4[E_1]_o[L]_o} - Q \quad (19)$$

$$\epsilon = \sqrt{Q^2 + 2Q([E_1]_o + [L]_o) + ([E_1]_o - [L]_o)^2} - Q > 0$$

Since ϵ is always positive, eq 18 indicates that k_+ is almost directly proportional to $[E_2]_o$ with a coefficient of k_5. As $[E_2]_o \rightarrow \infty$, all of the initial $[E_1L]$ will be instantaneously converted to E_1LE_2. However, k_- has an upper limit as

$$\lim_{[E_2]_o \rightarrow \infty} k_- = k_7\sqrt{K_4^2 + 2K_4([E_1]_o + [L]_o) + ([E_1]_o - [L]_o)^2} \quad (20)$$

$$\frac{dQ}{d[E_2]_o} = \frac{K_3K_4}{(K_3 + [E_2]_o)^2} > 0$$

From eq 19

$$\frac{d\epsilon}{dQ} = \frac{[E_1]_o + [L]_o + Q}{\sqrt{([E_1]_o + [L]_o + Q)^2 - 4[E_1]_o[L]_o}} - 1 > 0$$

Therefore,

$$\frac{d\epsilon}{d[E_2]_o} = \frac{d\epsilon}{dQ}\frac{dQ}{d[E_2]_o} > 0$$

From eq 18 we have

$$\frac{dk_-}{d[E_2]_o} = \frac{1}{2}\left\{k_5\left[1 - \frac{k_5[E_2]_o + k_6 - k_8 - k_7\epsilon}{\sqrt{(k_5[E_2]_o + k_6 - k_8 - k_7\epsilon)^2 + 4k_6k_8}}\right] + k_7\frac{d\epsilon}{d[E_2]_o}\left[1 + \frac{k_5[E_2]_o + k_6 - k_8 - k_7\epsilon}{\sqrt{(k_5[E_2]_o + k_6 - k_8 - k_7\epsilon)^2 + 4k_6k_8}}\right]\right\} \quad (21)$$

Therefore,

$$\frac{dk_-}{d[E_2]_o} > 0$$

In other words, both k_+ and k_- will increase as $[E_2]_o$ increases, and only k_- will reach a plateau when $[E_2]_o \rightarrow \infty$.

The theoretical treatment described above concludes that only the dissociative mechanism, and not the associative mechanism, can yield a kinetic pattern with a decreasing k_{app} as $[E_2]_o$ increases.

Results and Discussion

Predicted Kinetic Patterns from the Analytic Equations. Figure 1 shows the kinetic patterns obtained for a dissociative (Figure 1a) and for an associative (Figure 1b) mechanism, using both the analytic equations and numerical analysis. In both Figure 1 panels a and b, the solid curves were obtained by numerical solution using the MLAB numerical integration method. In the case of the dissociative mechanism, analysis of eq 8 reveals that the values of k_{app} (k_-), a pseudo-first-ordered rate constant for E_2L formation, can either decrease or increase as the initial concentration of E_2 approaches ∞. When $k_4 \geq k_2$, the value of δ (eq 12) will be larger than 0, and a decreasing pattern will be obtained. However, if $k_4 < k_2$, one can obtain either a decreasing or an increasing pattern, depending on the relative values for the first and second term in eq 12. It should be pointed out that at low $[E_2]_o$ the time course initially deviates from first-order rate law in numerical solutions. In addition, since eq 8 was solved with the assumption that the reactions are close to their equilibrium states in order to neglect the second-ordered terms, the time course was analyzed after the 1.3 half-life has been completed for the data shown in Figure 1a. Note that, as predicted, the deviation between the analytic solution, which is based on the approximation of small perturbations, and the numerical solution decreases as the reaction approaches equilibrium. In the case of an associative mechanism (Figure 1b), eqs 18 and 21 predicted that k_{app} (k_-) can only increase with increasing $[E_2]_o$ and reaches a plateau at a value shown in eq 20. Note that this value is always larger than the rate constant for the dissociation of E_1 from E_1LE_2 complex, and it is not equal to the off-rate constant of E_1 from E_1L complex. Similar to Figure 1a, Figure 1b shows that the results obtained using both the numerical and analytical solutions are in reasonable agreement. This agreement is further improved when the reaction closely approaches equilibrium, which is dictated by the assumption used in deriving the analytical solution.

Analysis of the Kinetic Patterns Displayed by Two Glycolytic Enzymes. The kinetics of the transfer of NADH between its complexes with glycerol-3-phosphate dehydrogenase (GPDH; EC 1.1.1.8) and with L-lactate dehydrogenase (LDH; EC 1.1.1.27) have been used as supporting evidence for the proposed substrate channeling in glycolysis (Srivastava & Bernhard, 1986a,b, 1987). Reexamination of this evidence revealed that the conclusion was based on misinterpretation of the kinetics of ligand exchange (Chock & Gutfreund, 1988; Wu et al., 1991). In our experiments, the transient kinetics for the transfer of NADH between the two dehydrogenases was measured at 10 °C using a Hi-Tech stopped-flow spectrometer as described earlier (Wu et al., 1991). The reactions were carried out in 50 mM HEPES buffer (pH 7.5) containing 1 mM β-mercaptoethanol, 1 mM EDTA, and 100 mM KCl. Figure 2 shows the observed first-order rate constants plotted as a function of $[E_2]_o$. Note that when E_1 and E_2 are LDH and GPDH from rabbit muscle, respectively, k_{app} increases with increasing $[E_2]_o$ (Figure 2a),

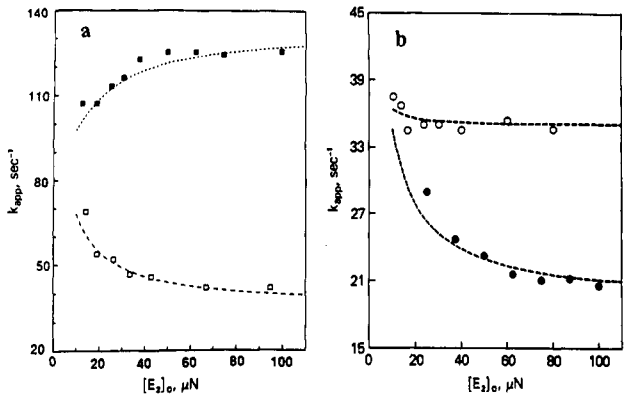

FIGURE 2: Correlation between pseudo-first-order rate constants for displacement of E_1 from its NADH complex by E_2 and $[E_2]_o$. The initial concentration of E_1 and NADH were 7.5 (subunit concentration) and 5 μM, respectively. The data were fitted to reactions 22 and 23 by the numerical integration method using the rate constants given in the text. (a) E_1 and E_2 are rabbit muscle LDH and GPDH or vice versa. The data (■) and (□) were obtained with E_2 being GPDH and LDH, respectively. (b) E_1 and E_2 are porcine heart muscle LDH and rabbit muscle GPDH or vice versa. The symbols (●) and (○) represent data obtained with E_2 being GPDH and LDH, respectively.

while in the case where E_1 and E_2 represent GPDH and LDH, respectively, or when porcine heart LDH was paired up with rabbit muscle GPDH (Figure 2b), decreasing patterns were observed.

The data in Figure 2 can be explained quantitatively with a dissociative mechanism. Kinetics of NADH binding to GPDH (rabbit muscle) and to LDH from rabbit muscle or porcine heart muscle show that the binding reactions are consistent with the following mechanistic schemes:

$$\text{GPDH} + \text{NADH} \underset{k_{10}}{\overset{k_9}{\rightleftharpoons}} \text{GPDH·NADH} \qquad (22)$$

$$\text{LDH} + \text{NADH} \underset{k_{12}}{\overset{k_{11}}{\rightleftharpoons}} \text{LDH*·NADH} \underset{k_{14}}{\overset{k_{13}}{\rightleftharpoons}} \text{LDH·NADH} \qquad (23)$$

where k_9 and k_{10} were determined to 0.41×10^8 M^{-1} s^{-1} and 35 s^{-1}, respectively (Wu et al., 1991). In the case of LDH, one cannot directly evaluate all of the rate constants, except for $k_{13} + k_{14}$, $k_{12}k_{14}/(k_{12} + k_{13})$, and $k_{11}/(k_{12} + k_{13})$, which were determined to be 1.7×10^3 s^{-1}, 125 s^{-1}, and 5.6×10^4 M^{-1} for rabbit muscle LDH and 540 s^{-1}, 18 s^{-1}, and 6.3×10^4 M^{-1} for porcine heart LDH, respectively. With these values and a numerical integration method, k_{11} was varied to fit the lower curve in Figure 2a. The value of k_{11} so calculated is 3×10^8 M^{-1} s^{-1}. With this information, one obtains k_{12}, k_{13}, and k_{14} to be 3831 s^{-1}, 1557 s^{-1}, and 176 s^{-1}, respectively, for the rabbit muscle LDH. Using the same set of rate constants, the initial concentration of the reactants, and a dissociative mechanism, one obtains the two calculated curves given in Figure 2a, which fit well to the experimental data. Furthermore, assuming the rate constant (k_{11}) for forming the collision intermediate is also equal to 3×10^8 M^{-1} s^{-1} for the porcine heart system, one obtains the values of k_{12}, k_{13}, and k_{14} to be 4235 s^{-1}, 516 s^{-1}, and 21 s^{-1}, respectively, for porcine heart LDH. As shown in Figure 2b, the calculated curves, based on a dissociative mechanism, again fit well with the experimental data obtained with rabbit muscle GPDH and porcine heart LDH as E_1 and E_2 or vice versa.

It should be pointed out that the apparent rate constants for NADH off-rate determined above is consistently lower by about 40–50% compared to those determined by NAD or adenosine 5′-diphosphoribose (Wu et al., 1991). This discrepancy, although relatively small, may derive from the effect

of nonspecific binding of NAD or adenosine 5'-diphosphoribose to the enzyme because the concentrations used are relatively high.

Possible Contribution from the Associative Mechanism. In an attempt to show the effect on the kinetic patterns due to contributions from both an associative and a dissociative mechanism to a given reaction, we analyzed the recent data reported by Srivastava et al. (1989). Using the NAD displacement method, Srivastava et al. obtained $k_{10} = 135\ s^{-1}$ and $k_{16} = 95\ s^{-1}$ for reactions 22 and 24, where NADH binding

$$\text{LDH} + \text{NADH} \underset{k_{16}}{\overset{k_{15}}{\rightleftharpoons}} \text{LDH·NADH} \qquad (24)$$

to LDH was treated as a one-step reaction. From these constants and the equilibrium constants, k_9 and k_{15} were calculated to be $1.69 \times 10^8\ M^{-1}\ s^{-1}$ and $1.86 \times 10^8\ M^{-1}\ s^{-1}$, respectively. Using these rate constants and a dissociative mechanism, one fails to fit the enzyme displacement data of Srivastava et al. (1989). Figure 3a,b shows that the curves (curve 1 in each case) calculated using the dissociative model are significantly higher though almost parallel to the observed data.

Since their k_{app} vs $[E_2]_o$ shows a decreasing pattern, an associative mechanism alone can be ruled out for the displacement reactions. The data were then analyzed using a model which combined both the dissociative and the associative mechanisms. The formation of the ternary complex can be accomplished by either reaction 25 or 26.

$$\text{GPDH·NADH} + \text{LDH} \underset{k_{18}}{\overset{k_{17}}{\rightleftharpoons}} \text{GPDH·NADH·LDH} \qquad (25)$$

$$\text{LDH·NADH} + \text{GPDH} \underset{k_{20}}{\overset{k_{19}}{\rightleftharpoons}} \text{GPDH·NADH·LDH} \qquad (26)$$

Using the rate constants of Srivastava et al. and the thermodynamic constraint, we have

$$\frac{k_{17}k_{20}}{k_{18}k_{19}} = \frac{k_{15}k_{10}}{k_{16}k_9} = 1.56 \qquad (27)$$

With this relationship, the values of k_{17} to k_{20} were selected to best fit the experimental data using the combined model and the numerical method. No improvement could be attained relative to the dissociative model alone. In general, independent of the rate constants selected within the constraint shown in eq 27, once the contribution from the associative mechanism becomes significant, the k_{app} exhibits an upward trend. In this case, the K_d for the GPDH·NADH·LDH complex was set at 50 or 100 μM, a lower limited value estimated from sedimentation equilibrium and gel filtration experiments (Wu et al., 1991). Note that curves 2 to 4 of Figure 3a,b were calculated with the combined model. Curve 2 in Figure 3a,b was calculated with $K_d = 100\ \mu M$ for eq 25 and letting $k_{17} = 1 \times 10^6\ M^{-1}\ s^{-1}$ and $k_{18} = 100\ s^{-1}$, and they show significant deviation from their respective curve 1. When one speeds up the enzyme–enzyme complex equilibrium by 50% in each direction, the resulting curve 3 in Figure 3a,b deviates further away from the experimental data and the respective curve 1. Curve 4 in Figure 3a,b was obtained with $K_d = 50\ \mu M$. In all cases, the calculated curves 2–4 exhibit further deviation from the observed data than curves calculated with a dissociative model alone (curve 1). The fractional contribution from the associative mechanism for curve 2 in Figure 3a,b is shown in Figure 3c as curves 2 and 1, respectively. Together they demonstrate that the extent of deviation increases as the fractional contribution from the associative mechanism increases, even though the associative pathway contributes only less than 17% of the total E_2·NADH formation at the highest

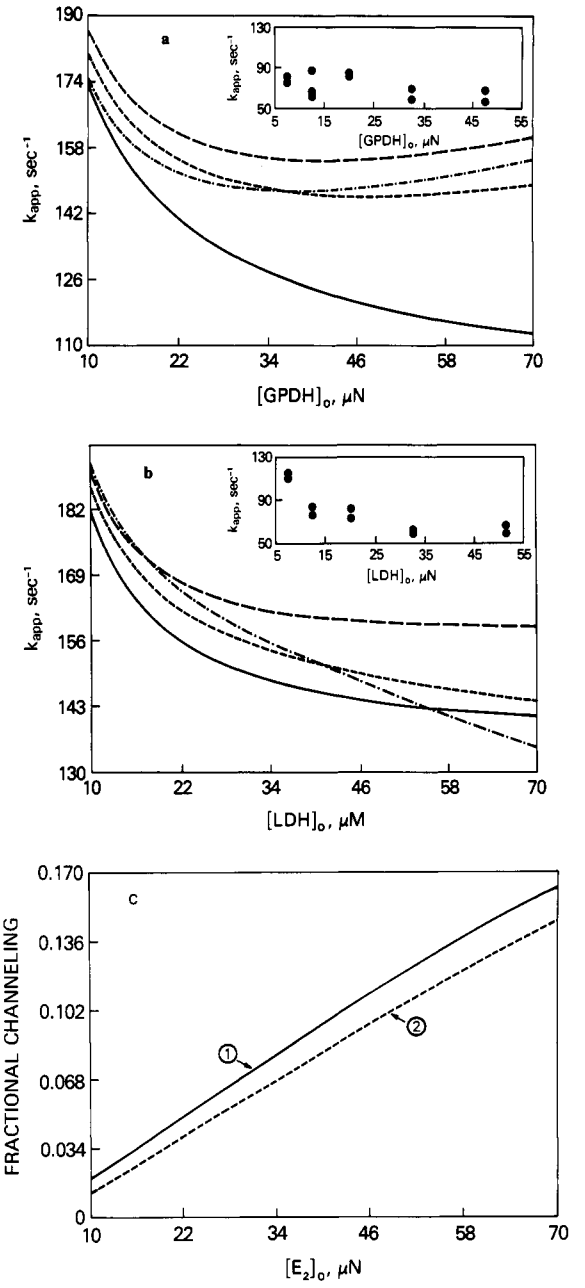

FIGURE 3: Comparative studies between an associative, a dissociative, and a mixed associative–dissociative mechanism relative to the experimental data of Srivastava et al. (1989). (a and b) Displacement of E_1 from E_1·NADH complex by E_2 with $[E_1]_o = 10\ \mu N$ (subunit concentration) and $[NADH]_o = 7.5\ \mu M$. Experimental data from Srivastava et al. (1989) for the same conditions are shown in insets. Curve 1 (—) is numerical simulation results using a dissociative model and the rate constants reported by the authors. Curve 2 (- - -), curve 3 (– – –), and curve 4 (–·–) were from numerical simulations using a combined model and an assumption that $k_{18} = k_{20}$ (see reactions 25 and 26) and the thermodynamic constraint (eq 27) holds. (Curve 2) $k_{17} = 10^6\ M^{-1}\ s^{-1}$ and $k_{18} = 100\ s^{-1}$; (curve 3) $k_{17} = 1.5 \times 10^6\ M^{-1}\ s^{-1}$ and $k_{18} = 150\ s^{-1}$; and (curve 4) $k_{17} = 10^6\ M^{-1}\ s^{-1}$ and $k_{18} = 50\ s^{-1}$. (a) E_1 = LDH, E_2 = GPDH, and [NADH] ($t = 0$) = 0.574 μM, [E_1] (0) = 3.074, and [E_1·NADH] (0) = 6.926 μN. (b) E_1 = GPDH and E_2 = LDH, with [NADH] (0) = 0.809 μM, [E_1] (0) = 3.309, and [E_1·NADH] (0) = 6.691 μN. (c) Fractional contribution of the channeling mechanism in the combined model. Curve 1 was calculated from curve 2 in panel b; curve 2 was calculated from curve 2 in panel a.

$[E_2]_o$ calculated. When the stability of the bienzyme was increased, e.g., by setting K_d equal or less than 50 μM, one obtained kinetic patterns which are less favorable to match the experimental data (see curve 4 in Figure 3a,b). Under

these conditions, the contribution from the associative pathway also increases (data not shown). In other words, the extent of the deviation of the kinetic pattern from the experimental data appears to be correlated with the increasing contribution of the associative pathway.

In conclusion, we have demonstrated that using a linearization assumption (Eigen & DeMaeyer, 1963) one can obtain analytical expressions for the kinetics of ligand substitution reactions. Analysis of these equations reveals that the kinetic patterns of the observed pseudo-first-ordered rate constants as a function of increasing concentration of the incoming ligand can differentiate an associative from a dissociative mechanism. An associative mechanism can only generate an increasing kinetic pattern, and it plateaus, in most cases, at a value larger than the off-rate constant of the leaving ligand. A dissociative mechanism can yield either an increasing or a decreasing kinetic pattern depending on the magnitude of the individual rate constants involved. In either case, the k_{app} plateaus at a value equal to the off-rate constant of the leaving ligand. In other words, an observed decreasing kinetic pattern is indicative that the reaction proceeds via a dissociative mechanism. It should be pointed out that, using the numerical simulation method, one can easily obtain kinetic patterns based on a given mechanistic scheme and a set of rate constants. However, the analytical expressions shown here provide the theoretical basis for the arguments described above, and they allow one to generalize the method for differentiating mechanisms for ligand exchange reactions. We have applied this general method to analyze the data reported by Srivastava et al. (1989) and our data on the transfer of NADH between its complexes with GPDH and with LDH. The results showed that the transfer of NADH between these enzymes proceeds via a dissociative mechanism.

References

Chock, P. B., & Gutfreund, H. (1988) *Proc. Natl. Acad. Sci. U.S.A. 85*, 8870–8874.

Eigen, M., & DeMaeyer, L. (1963) in *Techniques of Organic Chemistry* (Friess, S. L., Lewis, E. S., & Weissberger, A., Eds.) Vol. VIII, Part 2, pp 895–1054, Wiley Interscience, New York.

Knott, G. D. (1979) MLAB—A Mathematical Modeling Tool, *Comput. Programs Biomed. 10*, 271–280.

Srivastava, D. K., & Bernhard, S. A. (1986a) *Science 234*, 1081–1086.

Srivastava, D. K., & Bernhard, S. A. (1986b) *Curr. Top. Cell. Regul. 28*, 1–68.

Srivastava, D. K., & Bernhard, S. A. (1987) *Biochemistry 26*, 1240–1246.

Srivastava, D. K., Smolen, P., Betts, G. F., Fukushima, T., Spivey, H. O., & Bernhard, S. A. (1989) *Proc. Natl. Acad. Sci. U.S.A. 86*, 6464–6468.

Wu, X., Gutfreund, H., Lakatos, S., & Chock, P. B. (1991) *Proc. Natl. Acad. Sci. U.S.A. 88*, 497–501.